ELLIPSOMETRIC STUDIES OF POLYCRYSTALLINE MOLYBDENUM SILICIDE THIN FILMS

G. Srinivas* and V.D. Vankar
Thin Film Laboratory, Department of Physics,
Indian Institute of Technology, Delhi, India

(Refereed)
(Received June 21, 1996; Accepted July 19, 1996)

ABSTRACT

Systematic ellipsometric studies of $MoSi_2$ (tetragonal) thin films formed by RTA processing of cosputtered $Mo_{25}Si_{75}$, $Mo_{30}Si_{70}$, and $Mo_{36}Si_{64}$ thin films are discussed. The optical properties of these films in the measured spectral range 1.3–5.3 eV were observed to be dominated by the microstructural variations such as due to the changes in density, oxide overlayer thickness and composition, surface roughness, and redistribution of available excess silicon (after formation of $MoSi_2$ (tetragonal) phase). These microstructural variations indicated modification of interfaces and significant change in conductivity, which were corroborated in the AES depth profiles and the electrical resistivity measurements.

KEYWORDS: A. thin films, B. sputtering, D. optical properties

INTRODUCTION

Silicide thin films have low resistivity and high thermal stability and find application in VLSI as contacts, interconnects, and gates (1–12). The optical properties of materials in the range near IR to near UV spectral region are determined by the electronic polarizabilities, which, in turn, are determined by the kind of atoms present, their bonding configurations and density, and the presence or absence of long-range order. The study of optical properties

thus provides a nondestructive fingerprinting technique for understanding the microstructural information of materials as well as an insight into the electronic band structure of these materials. The optical properties of some silicides, such as nickel, chromium, cobalt, and molybdenum, are available in the literature. However, the emphasis of previous studies was on acquiring accurate spectral data and comparison with metal counterparts (13–22). Ged et al. (18) studied the optical properties of single crystal $MoSi_2$ and observed anisotropy effects in the dielectric spectra. The anisotropy effects were explained on the basis of the differences in the valence band density of states, which pointed to Mo 'd' electrons being strongly coupled with Si 'p' ones along (a,b) directions, rather than along c direction. Similar anisotropic effects were reported by Ferrieu et al. (19) in WSi_2 and $MoSi_2$ single crystals.

In this article, we discuss the systematic ellipsometric studies of $MoSi_2$ thin films and the microstructural details that can be drawn from the optical properties of these films. The microstructural variations indicated changes in conductivity and interface broadening due to redistribution of excess silicon available after the formation of $MoSi_2$(t) phase and were corroborated with our observations from AES depth profiles and resistivity measurements.

EXPERIMENTAL PROCEDURE

Thin films of compositions $Mo_{25}Si_{75}$, $Mo_{30}Si_{70}$, and $Mo_{36}Si_{64}$ were cosputtered onto p-type silicon substrates in a vacuum system evacuated to an ultimate pressure of 1×10^{-6} torr. The process pressure was 4×10^{-2} torr, while the power applied to the targets was varied to obtain the desired film composition. The as-deposited thin films of desired compositions in which the impurity levels of carbon and oxygen are less than 3 atomic percent were annealed using a rapid thermal annealing system (Heat Pulse 210T model, A.G. Associates, USA) in the temperature range 750–1150°C for 30 seconds in argon atmosphere. The samples were later analyzed for the formation of the most stable $MoSi_2$ tetragonal phase using X-ray diffraction technique and were further characterized by ellipsometry. The optical properties of these thin films were studied using a rotating-polarizer-type spectroscopic ellipsometer (Sopra ES2G, make France) in the range 1.3–5.3 eV. Bruggeman effective medium approximation was used extensively to understand the microstructural details of the polycrystalline $MoSi_2$ tetragonal films.

RESULTS AND DISCUSSION

The optical properties of crystalline materials are understood more clearly in terms of interband transitions observed in ε_2 spectra. Figure 1 illustrates the typical spectral dependence of ε_2 for $MoSi_2$(t) films formed by annealing as-deposited films of compositions $Mo_{25}Si_{75}$ and $Mo_{36}Si_{64}$ at two annealing temperatures (about 1050°C and 1150°C). We observed major peaks centered around 1.4, 2.5, and 3.4 eV. The exact peak positions observed in the ε_2 spectra of $MoSi_2$(t) films formed by RTA annealing of the as-deposited films are tabulated in Table 1.

The $MoSi_2$(t) films formed out of $Mo_{25}Si_{75}$ by annealing at 1000°C exhibited maxima at 1.54, 1.76, 2.50, 2.70, and 3.44 eV, whereas those formed at higher annealing temperatures (about 1100°C) showed maxima at 1.49, 1.76, 2.43, and 2.66 eV. It should be

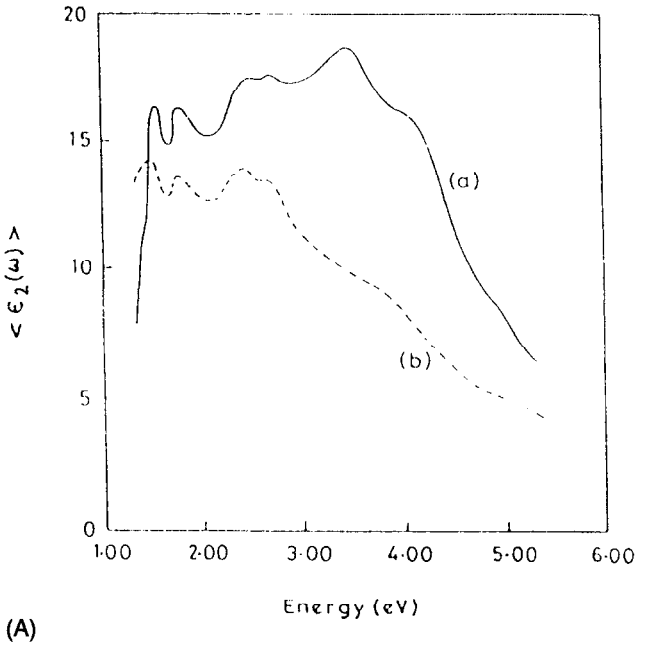

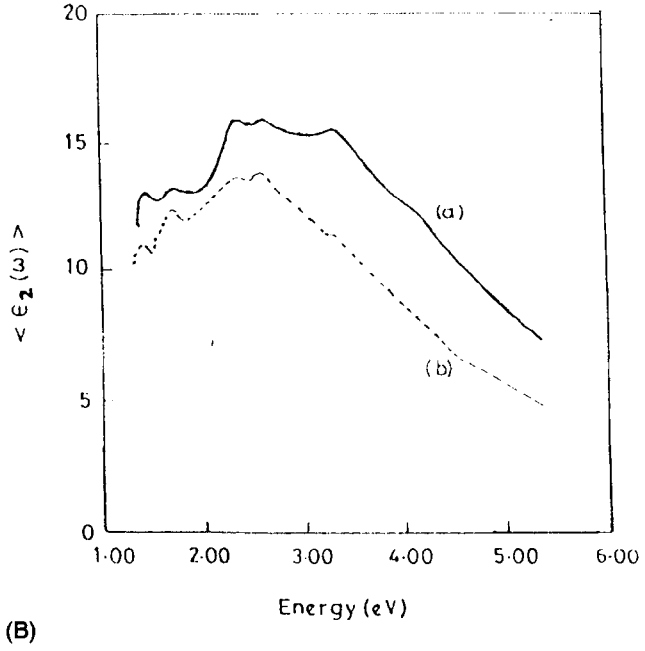

FIG. 1

The spectral dependence of ε_2 for polycrystalline $MoSi_2$ (tetragonal) thin films formed by RTA processing of as-deposited films of composition (A) $Mo_{25}Si_{75}$, annealed at (a) 1000 and (b) 1100° and (B) $Mo_{36}Si_{64}$ annealed at (a) 1050 and (b) 1150°C.

TABLE 1
The Positions of Maxima in ε_2 Spectra of $MoSi_2$(t) Films Formed by RTA Annealing of As-Deposited Films of Composition $Mo_{25}Si_{75}$, $Mo_{30}Si_{70}$, and $Mo_{36}Si_6$, and $MoSi_2$(x-tal), Mo and Si

As-deposited composition	Annealing temperature (°C)	ε_2 Peak positions (eV)
$Mo_{25}Si_{75}$	1000	1.54, 1.76, 2.50, 2.70, 3.44
	1100	1.49, 1.74, 2.43, 2.66
$Mo_{30}Si_{70}$	1050	1.48, 1.74, 2.43, 2.64, 3.44
	1150	1.45, 1.74, 2.40, 2,58, 3.81 (w)*
$Mo_{36}Si_{64}$	1050	1.46, 1.72, 2.41, 2.61, 3.35
	1150	1.45, 1.70, 2.36, 2.58, 3.35 (w)
$MoSi_2$(x-tal) (18)	*a* and *b* axes	1.32, 2.47, 3.8
	c axis	1.32, 2.58
$MoSi_2$ (19)	Polycrystalline film	2.45, 2.60, 3.75, 4.15
Mo	x-tal	1.7, 2.3
Si	x-tal	3.4, 4.5

*w = weak peak

noted that the 3.44 eV peak observed for films annealed at lower temperature (1050°C) is conspicuously absent for the films annealed at high temperature (1150°C). The maxima in the ε_2 spectra of $MoSi_2$(t) films formed by annealing films of composition $Mo_{30}Si_{70}$ at 1050°C were observed at 1.48, 1.74, 2.43, 2.64, and 3.44 eV, whereas in the case of high-temperature (1150°C) annealed samples, the maxima were observed at 1.45, 1.74, 2.40, and 2.58 eV and a weak maximum at 3.81 eV. The ε_2 peak observed around 3.4 eV in low-temperature annealed samples is not present for high-temperature annealed samples, instead a weak peak at 3.81 eV is observed. The ε_2 spectra of $MoSi_2$(t) samples formed by annealing films of composition $Mo_{36}Si_{64}$ at 1050°C exhibited maxima at 1.46, 1.72, 2.41, 2.61, and 3.35 eV, whereas the $MoSi_2$(t) samples obtained by annealing films of the same composition at a relatively higher temperature (1150°C) exhibited maxima at 1.45, 1.70, 2.36, and 2.58 eV and a weak maximum at 3.35 eV. Thus, we can see that the ε_2 peak positions have shifted to lower energies along with an associated decrease in peak height with increase in the annealing temperatures for all these compositions. Further, the magnitude of ε_2 values of $MoSi_2$(t) thin films decreases with the decrease in silicon content of as-deposited thin films and show a corresponding shifts to lower energies.

The ε_2 spectra of monocrystalline $MoSi_2$ by Ged et al. (18) showed maxima at 1.32, 2.58 and 3.82 eV along *c* axis and maxima at 1.32, 2.47 eV along *a* and *b* axes. The ellipsometric studies of Henrion et al. (21) on cosputtered silicide thin films of molybdenum silicide exhibited maxima at 2.40, 2.62, and 3.10 eV in the ε_2 spectra. Ferrieu et al. (19) reported maxima in ε_2 spectra of $MoSi_2$(x-tal) around 2.45 and 4.1 eV along *a* and *b* axes and at 2.60 and 3.75 eV along *c* axis. The peak positions can be understood by comparing with the

standard ε_2 spectra of elemental molybdenum and silicon. The ε_2 spectrum of molybdenum shows maxima at 1.70 and 2.3 eV. The ε_2 spectrum of crystalline silicon shows maxima at 3.4 and 4.5 eV. The low energy features of ε_2 observed by Ged et al. in the monocrystalline $MoSi_2$ around 1.3 and 2.5 eV were predicted to be due to Mo 'd' electrons, whereas those in the monocrystalline $MoSi_2$ around 4 eV are Si 'p' electron derived with contributions from Mo 'd' electrons. The structure around 4 eV was reported to be strongly anisotropic and appears preferentially for the direction $\vec{E}$ perpendicular to $\vec{C}$ direction. By considering the fact that the differences in the valence-band density of states, they explained the preferential 3.8 eV peak for a,b directions to be due to strong coupling between Mo 'd' electrons with the Si 'p' electrons along a,b directions than along c direction.

The experimental studies by Weaver et al. (22) on the electronic band structure exhibit maxima in the photoelectronic spectroscopy at 2.2, 5.8, 7.5–8.0, and 11 eV below E_F. They concluded that the electronic structure of $MoSi_2$ is dominated by metal-d derived character within 5 eV of the Fermi level and that the Si 's' and 'p' derived bands extend to 12 eV below E_F. The peak at 2.2 eV has been associated with the contributions due to metal 'd' bands and as excitation of electrons from metal 'd' bands to the Fermi level (E_F). The theoretical calculations of the band structure of $MoSi_2$ by Bhattacharya et al. (23) exhibited maxima in the density of states (DOS) at 2.35 and 6.1 eV below E_F. The loss peak at 3.9 eV observed in the EELS spectra by Rastogi et al. (24) was associated with the excitation of electrons from Mo(4d)-Si(3p) levels to the Fermi level (E_F).

The major factors contributing to changes in the ε_2 spectrum are surface roughness, density changes, surface oxidation, and changes in compositional order. The surface morphology studies (SEM micrographs) of our films exhibited increasing roughness with increase in annealing temperature. The stress measurements discussed elsewhere (25) indicated an increase in stress with increase in annealing temperature. Though grain size measurements were not undertaken, we expect an increase in grain size with increase in the annealing temperature. The decrease in the ε_2 values in the $MoSi_2$(t) films with the increase in annealing temperature we observed in all samples (formed out of various compositions, $Mo_{25}Si_{75}$, $Mo_{30}Si_{70}$, and $Mo_{36}Si_{64}$, by annealing) could be due to the increase in surface roughness, grain size, or stress, or all of these to varying extent.

The loss of the silicon-derived 3.4 eV peak observed in the case of $MoSi_2$(t) thin films formed out of $Mo_{25}Si_{75}$ and $Mo_{30}Si_{70}$ with increase in annealing temperature, or the suppression of 3.81 eV peak in the case of films formed out of $Mo_{36}Si_{64}$, with increase in annealing temperature cannot be accounted for by the increase in surface roughness alone. During the annealing process it is very likely that an overlayer of SiO_2 of small thickness grows on the film, which may contribute to changes in ε_2 spectra. The kinetics of SiO_2 growth by thermal annealing of $MoSi_2$ films on SiO_2 substrates in dry oxidation ambient is reported to follow the relation, $x^2 + Ax = B(t + \tau)$, where x is the thickness, t is time, and B/A is the rate constant. The oxide thickness grown on $MoSi_2$ upon annealing at 900°C for 1 h in dry ambient is reported to be about 200 Å (11). The thickness of oxide grown on our films in the RTA process is expected to be about 50 Å and is not expected to change much by increasing the annealing temperature from 1050 to 1150°C. We, therefore, cannot associate the loss of 3.4 eV with increase in oxide formation alone. Because our films are polycrystalline and X-ray diffraction results do not show any changes associated with preferred orientation effects with increase in annealing temperature from 1000 to 1150°C, we rule out the anisotropy contribution to the changes observed in ε_2 spectra for the above discussed films.

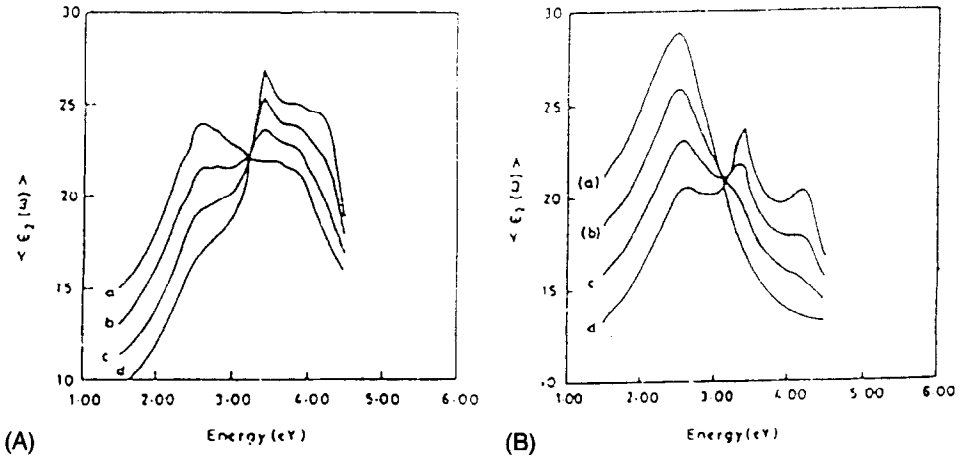

FIG. 2

Simulated ε_2 spectra along (A) a,b direction and (B) c direction for $MoSi_2$ (x-tal) with random mixture of various fractions of silicon: 0%,10%, 20%, 30% (a,b,c,d).

To draw the microstructural details from the dielectric function, a fair knowledge of the effects of the microstructural inhomogenities such as voids, surface roughness, and the random segregation of an element in a matrix is required. The discussion that follows describes the simulation of such effects and compares with our experimental observations. The Bruggeman effective medium model was used as the basis for this simulation. We have used the data on single crystals reported by Ged et al. for the spectral response of the $MoSi_2$ (x-tal) for these simulations.

The most common type of the microstructural variations observed in most of vapor-deposited films are voids. Because the dielectric function is defined as the polarization per unit volume, it clearly reflects the fraction of voids in it. Voids may be described as bulk density deficiency in a material and therefore their volume fraction can be calculated using effective medium theories by assuming them to be a phase with $\varepsilon_1 = 1$ and $\varepsilon_2 = 0$ in the multiphase microstructural modeling. Because the magnitude of the dielectric a constant peak is dependent on the density of the material, any decrease in the ε_{2max} peak without shift in the peak position could be treated as due to the presence of voids and the fraction of voids can be calculated relative to the films or quantitatively in any film with respect to a void-free bulk sample. Another microstructural variation commonly reflected in the surface morphology is the surface roughness. An increase in surface roughness is reflected as a decrease in the value of ε_{2max} accompanied by a shift of the peak position towards lower energy.

Figure 2 simulates the effect of random mixture of silicon in the matrix of $MoSi_2$. With the increasing fraction of silicon randomly mixed in $MoSi_2$ (x-tal) along a,b direction, we can observe that the height of 2.58 eV peak decreases without any associated peak shifts. The 3.82 eV peak, however, increases in height with increase in the fraction of silicon. In addition, two new peaks appear, one around 3.4 eV and the other around 4.3 eV. In the case of $MoSi_2$ (x-tal) along c direction, molybdenum derived peak at 2.47 eV shifts to higher energies with an associated decrease in peak height, with increase in silicon fraction. The silicon-derived peaks at 3.4 and 4.3 eV shift marginally toward higher energies, with increase in silicon fraction. The oxide overlayers on the substrates or thin films are

unintentional and sometimes unwanted surface modifications. The presence of an oxide overlayer on Si substrates (most commonly used substrates in the semiconductor industry) is reflected on the dielectric constant by reducing ε_{2max} peak height associated with a peak shift. A multilayer model based on a simple relation given by Aspnes could be used to study the oxide overlayers (25).

Figure 3 simulates the effect of a silicon-dioxide overlayer on $MoSi_2$. Because SiO_2 is transparent in the spectral region of our interest, no new peaks were introduced by increasing the SiO_2 thickness; however, the magnitude of ε_{2max} increases up to 2.35 eV in $MoSi_2$ (x-tal) along a,b direction and up to 2.15 eV along c direction. Beyond this the magnitude of ε_2 decreases with increase in thickness of oxide overlayer and the position of the maxima shift to lower energies. We also observe that the silicon derived 3.82 eV peak of $MoSi_2$ (x-tal) along a,b direction shifts to higher energies and becomes insignificant for an oxide thickness above 30 Å.

These simulation results were taken as guidelines in modeling the microstructural details of our silicide thin films. Because the $MoSi_2$(t) thin films formed were polycrystalline in nature and $MoSi_2$(x-tal) exhibits anisotropy in dielectric response (18), a reasonable fraction of this anisotropy is required to be accommodated. Ferrieu et al., in a similar study on polycrystalline WSi_2 thin films, showed that a reasonable fit with experimental data could be obtained if $\langle\varepsilon\rangle = 1/3\varepsilon_{ac} + 2/3\varepsilon_{ab}$, where ε_{ab} and ε_{ac} correspond to single crystal measurements along *b* and *c* axes, respectively (15). Our experimental results were analyzed according to this relationship. However, our results did not fit well with this approximation. Our simulation results indicated that $\langle\varepsilon\rangle = 1/5\varepsilon_{ac} + 4/5\varepsilon_{ab}$ gave a best fit over the measurements of the polycrystalline $MoSi_2$(t) thin films chosen in the present study. As no distinct orientational changes were observed in the GAXRD patterns of these films annealed at 1050 and 1150°C, we do not expect any significant change in the qualitative interpretation of the data with this assumption.

The microstructural modeling discussed in detail elsewhere (27) clearly give an insight into the kinetics of silicide formation. The reaction products of silicon-rich silicide thin films

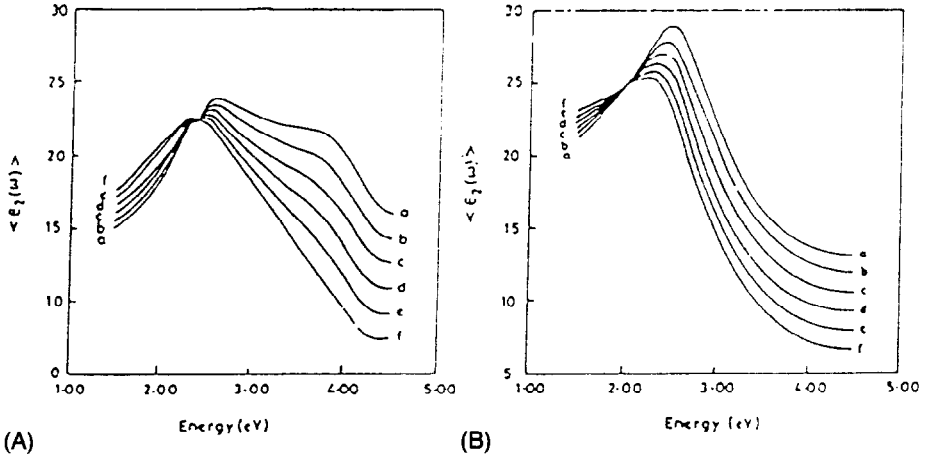

FIG. 3

Simulated ε_2 spectra along (A) a,b direction and (B) c direction for various thicknesses of SiO_2 on $MoSi_2$ (x-tal): 0, 10, 20, 30, 40, 50 Å (a,b,c,d,e,f).

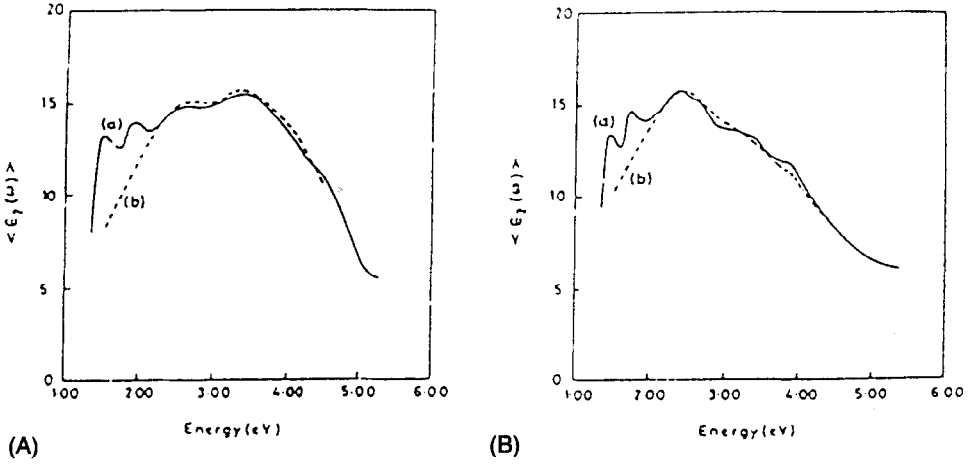

FIG. 4

Best fit microstructural modeling curves (a) (----) over experimental curves (b) (—) for $MoSi_2(t)$ thin films formed out of $Mo_{30}Si_{70}$ by RTA annealing at (A) 1050°C and (B) 1150°C .

(silicon deposited in excess of the stoichiometry) are $MoSi_2$ and silicon. The excess silicon available after the formation of $MoSi_2$ in the silicon-rich silicide thin films is randomly mixed in the $MoSi_2$ matrix at low temperatures, diffuses toward the interface of the substrate and the film, and recrystallizes at higher temperatures. Figure 4 illustrates the typical best fit microstructural modeling curves over the experimental curves for $MoSi_2(t)$ thin films formed out of $Mo_{30}Si_{70}$ by RTA annealing at 1050 and 1150°C. The microstructure of the $MoSi_2(t)$ thin films formed out of $Mo_{30}Si_{70}$ at 1050°C as modeled results in a first layer of polycrystalline $MoSi_2$ with silicon (19 ± 3%) and voids (21 ± 2%) and an overlayer of SiO_2 of thickness, 33 ± 6 Å with voids (9 ± 1%). The microstructure of the $MoSi_2(t)$ thin films formed at 1150°C as modeled shows a first layer of polycrystalline $MoSi_2$ with voids (20 ± 3%) and an overlayer of SiO_2 of thickness 45 ± 5 Å and voids (23 ± 1%). One can easily notice that silicon present in excess in the matrix of $MoSi_2(t)$ at low annealing temperatures moves toward the $MoSi_2$-substrate interface and that some of it has contributed to the formation of more SiO_2. The changes in the microstructure of the overlayer clearly reflects roughening upon annealing at higher temperature. It can be observed from Figure 4 that the best fit was observed for energy range 2 to 5 eV only. For lower energies (less than 2 eV), oscillations were observed in the experimental data. Such oscillations due to multi-reflection interferences were also noticed in the study of WSi_2 thin films by Ferrieu et al. (19), who considered them to be due either to over stoichiometry of the silicide or to the interface roughness introduced by the finite grain size and that the interferences are associated with the transparency of the material in this energy range. Because such oscillations were noticed in $MoSi_2(t)$ thin films formed out of all the compositions chosen, we attribute them to the interface roughness only.

The shift in the ε_2 peak positions to lower energies in these films with increase in annealing temperatures can be associated with the increase in conductivity. The increase in conductivity at higher annealing temperatures suggests a redistribution of excess silicon available after the formation of $MoSi_2(t)$ phase (due to the over stoichiometry in the as-deposited films and also that which diffuses out from the substrate due to annealing). The

observed AES depth profiles show broadening of the interfaces. The increase in conductivity with increase in annealing temperature in these samples is consistent with the electrical resistivity measurements, which indicate a decrease in resistivity with increase in annealing temperature.

The shift of ε_2 peak positions of $MoSi_2$(t) films, with decrease in silicon content of the starting compositions ($Mo_{25}Si_{75}$, $Mo_{30}Si_{70}$, and $Mo_{36}Si_{64}$) can be understood from the realization that the volume fraction of silicon available in excess after the formation of $MoSi_2$(t) phase decreases in going from $Mo_{25}Si_{75}$ to $Mo_{36}Si_{64}$. These shifts can be associated with an increase in conductivity of the $MoSi_2$(t) samples formed out of $Mo_{36}Si_{64}$ with respect to those formed out of $Mo_{25}Si_{75}$. The presence of excess silicon in the matrix of silicide at low annealing temperatures and its outdiffusion leading to recrystallization as an epitaxial layer on the substrate has been reported in many other silicide thin films (28–38). The resistivities of $MoSi_2$(t) formed out of $Mo_{25}Si_{75}$ at 1000 and 1100°C were 225 and 155 μΩ-cm, respectively. The resistivity of $MoSi_2$(t) formed out of $Mo_{30}Si_{70}$ at 1050 and 1150°C were 210 and 120 μΩ-cm, respectively, whereas those formed out of $Mo_{36}Si_{64}$ at 1050 and 1150°C were 155 and 95 μΩ-cm, respectively.

CONCLUSIONS

A systematic ellipsometry study of the of $MoSi_2$ (tetragonal) thin films formed by RTA processing of cosputtered $Mo_{25}Si_{75}$, $Mo_{30}Si_{70}$, and $Mo_{36}Si_{64}$ thin films was carried out in detail and the maxima observed corroborated with the published reports on the electronic band structure. The position of the maxima observed in the dielectric spectra and the associated shifts of the maxima with increase in annealing temperature indicated large variations in microstructure. The simulation studies, and the microstructural models developed thereby, indicated that the reaction products of these as-deposited films at low annealing temperatures (about 1050°C) were $MoSi_2$, voids, and silicon and at higher annealing temperatures (about 1150 °C) were $MoSi_2$ and voids. The modeling results predicted the void fraction in various silicide thin films to vary between 12% and 21% and an overlayer of SiO_2 of thickness about 50 Å over the silicide thin films.

REFERENCES

1. F. Mohammadi, *Solid State Technol.* **24**, 65 (1981).
2. G. Ottaviani and C. Nobili, *Thin Solid Films* **163**, 111 (1983).
3. G. Ottaviani, *J. Vac. Sci. Technol.* **16**, 1112 (1979).
4. A.K. Sinha, *J. Vac. Sci.Technol.* **19**, 778 (1981).
5. F.M. d'Heurle and P.S. Ho, in *Thin Films-Interdiffusion and Reactions*, ed. J.M. Poate, K.N. Tu and J.W. Mayer, Chap. 8, Wiley, New York (1978).
6. C. Canali, F. Catellanni, G. Ottaaviani and M. Prundeziati, *Appl. Phys.Lett.* **33**, 187 (1978).
7. R.J. Holwill, *Mat Sci.& Eng. A* 116, 143 (1989).
8. S.P. Murarka, in *Silicides for VLSI Applications*, p. 5, Academic Press, New York (1983).
9. A.N. Saxena and D. Pramanik, *Solid State Technol.* **27**, 93 (1984).
10. *Microelectronic Materials*, p. 197, ed. C.R.M. Grovenor Adam Hilger, Bristol, UK (1989).
11. M.A. Nicolet and S.S. Lau, in *Formation and Characterisation of Transition Metal Silicides* (VLSI Electronics–Materials and Process Characterisation), Vol. 6, Chap. 6, Academic Press, New York (1983).

12. P. Rosser and G. Tomkins, *Vacuum* **35**, 419 (1985).
13. C. Viguer, A. Cros, A. Humbert, C. Ferrieu, O. Thomas, R. Madar and J.P. Senateur, *Solid State Commn.* **60**, 923 (1986).
14. J.R. Jimenez, Z.C. Wu, L.J. Schowalter, B.D. Hunt, R.W. Fathauer, P. Grunthaner and T.L. Lin, *J. Appl. Phys.* **66**, 2738 (1989).
15. H.W. Chen and J.T. Lue, *J. Appl. Phys.* **59**, 2165 (1986).
16. M. Amiotti, A. Borghesi, C. Guiizzetti and F. Nava, *Phys. Rev. B* **42**, 8939 (1990).
17. J.-T. Lue, S-J. Mu and I.-C. Wu, *Phys. Rev. B* **36**, 1657 (1987).
18. Ph. Ged, R. Madar and J.P. Senateur, *Phys. Rev. B* **29**, 6981 (1984).
19. F. Ferrieu, C. Viguier, A. Cros, A. Humbert, O. Thomas, R. Madar and J.P. Senateur, *Solid State Commn.* **62**, 455 (1987).
20. O. Thomas, J.P. Senateur, R. Madar, O. Laborde and E. Rosencher, *Solid State Commn.* **55**, 629 (1985).
21. W. Henrion, G. Beddies and H. Lange, *Phys. Stat. Sol. B* **131**, K55 (1985).
22. J.H. Weaver, V. Moruzzi and F.A. Schmidt, *Phys. Rev. B* **23**, 2916 (1981).
23. B.K. Bhatttacharya, D.M. Bylander and L. Kleinmann, *Phys. Rev. B* **32**, 7973 (1985).
24. R.S. Rastogi, V.D. Vankar, M.C. Bhatnagar and K.L. Chopra, *J. Vac. Sci. Technol. A* **6**, 2957 (1988).
25. Krishan Lal, R. Mitra, G. Srinivas and V.D. Vankar, *J. Appl. Cryst.* **29**, 222 (1996).
26. D.E. Aspenes and A.A Studna, *Phys. Rev. B* **27**, 985 (1983).
27. G. Srinivas and V.D. Vankar, *Mater. Lett.*, in press.
28. S.P. Murarka and S. Vaidya, *J. Appl. Phys.* **56**, 3404 (1984).
29. H. Gant, H. Boetticher and H.R. Deppe, *J. Vac. Sci. Technol. B* **3**, 1668 (1985).
30. S. Vaidya, T.F. Retajczyk and R.V. Knoell, *J. Vac. Sci. Technol. B* **3**, 846 (1985).
31. A.E.T. Kuiper, G.C.J. Vander Ligt, W.M. Vande Wijgert, M.F.C. Willemsen and F.H.P.M. Habraken, *J. Vac Sci. Technol. B* **3**, 830 (1985).
32. C. Cohen, R. Nipoti, J. Siejka, G.G. Bentini, M. Berti and A.V. Drigo, *Appl. Phys. Lett.* **61**, 5187 (1987).
33. S. Inoue, N. Toyokura, T. Nakamura and H. Ishikawa, *J. Electrochem Soc.* **128**, 2402 (1981).
34. T.J. Magee, G.R. Woolhouse, H.A. Kawayashi, I.C. Niemeyer, B. Rodrigues, R.D. Ormond and A.S. Bhandia, *J. Vac. Sci. Technol. B* **2**, 756 (1984).
35. M. Eizenberg, H. Foell and K.N. Tu, *J. Appl. Phys.* **52**, 861 (1981).
36. M. Eizenberg and K.N. Tu, *Appl. Phys. Lett.* **37**, 547 (1980).
37. S. Kritzinger and K.N. Tu, *J. Appl. Phys.* **52**, 305 (1981).
38. R.W. Bower and J.W. Mayer, *Appl. Phys. Lett.* **20**, 359 (1972).